

DRAFT

OMAE2002-28062

AN ASSESSMENT OF EOF CURRENT SCATTER DIAGRAMS WITH RESPECT TO RISER VIV FATIGUE DAMAGE

Trond Stokka Meling, Statoil

Kenneth Johannessen Eik, Statoil

Einar Nygaard, Statoil

ABSTRACT

The accuracy of the current modelling is critical when considering deepwater riser fatigue damage caused by vortex-induced vibrations (VIV). In the present study the use of empirical orthogonal functions (EOF) to simplify huge amounts of current measurements has been assessed. The amplitudes of the time varying principal components (PC) have been organized into bins in scatter diagram. The accuracy of this scatter diagram approach with different numbers of EOF modes involved has been evaluated in terms of riser VIV fatigue damage.

INTRODUCTION

For deepwater risers the current is the governing environmental load, hence, the accuracy of the applied current distributions become increasingly important with water depth. Traditionally enveloping current profiles are used, i.e. based on current measurements at selected depths the corresponding velocity distributions are established independently at each depth, and current profiles with the desired return period can be found. Hence, spanwise coupling is disregarded and the established current profiles are unlikely to represent 'real' profiles. They might also be non-conservative. The latter has been shown in a paper by Adams and Thorogood (1998) where it is indicated that use of what they call *concurrent* profiles give fatigue lives an order of magnitude lower compared to conventional methods.

Current measurements at a field location generate huge amounts of data impractical to apply in any riser analyses. Hence, a method to extract the most important characteristics of a current dataset into a manageable level of current profiles is

very important for reliable riser analyses. When considering vortex-induced vibrations (VIV) of risers, the current velocity is of course important, but the spanwise coupling is equally important in terms of *power-in* regions. Power-in region is an expression common for semi-empirical VIV software codes, like SHEAR7 by Vandiver et al. (2002), reflecting the length of the region where an eigenfrequency will have a positive lift coefficient. Uniform current profiles typically give the longest power-in regions. Traditional envelope methods may give current profiles that are more sheared than in reality by neglecting spanwise coupling, resulting in shorter "power-in" regions and thereby less VIV fatigue damage.

Lately the use of empirical orthogonal functions (EOF) as a tool to simplify current data and derive design current profiles, has been presented by several authors, see e.g. Forristall and Cooper (1997) and Jeans and Feld (2001). However, the EOF method is not new and has been applied by the meteorologists and oceanographers for several decades to analyse complex time series. While the mentioned authors focused upon extreme current profiles, the present study assesses the accuracy of the EOF method in terms of riser VIV fatigue damage, i.e. the EOF current profiles are used as input to the VIV code SHEAR7 by Vandiver et al. (2002), to predict damage.

NOMENCLATURE

EOF	Empirical Orthogonal Functions
PC	Principal components
SVD	Singular Value Decomposition
VIV	Vortex-Induced Vibrations

THE EOF METHOD

The aim of EOF analysis is to provide a compact description of the spatial and temporal variability of data series in terms of orthogonal functions (also called statistical ‘modes’). They play the same role as sine waves do in ordinary Fourier spectral analysis. The data can be expressed as a sum of EOFs just as every time series can be expressed as a sum of sine waves.

It can be shown that the EOFs are the most efficient method of compressing the data. Here efficiency is used in the sense of lowest total mean square error. The EOFs are order so the first mode explained most of the variance in the data, and usually most of the variance in a data set can be explained by only a few orthogonal functions. Thus even large data sets may to a good approximation be reduced to typically 1-3 EOFs.

There are two main assumptions on which the EOF analysis is based. Firstly, that the time evolution of the dominant modes are uncorrelated. Secondly, that the dominant modes are orthogonal in space. Even if the first modes should correspond to different physical mechanisms, the time variation of these processes should further be uncorrelated, for the EOF analysis to give the "correct" result. As a result, a single physical process may often be spread over more than one EOF. In other cases more than one physical process may be contributing to the variance contained in a single EOF. Physical interpretation of the modes should therefore always be made with great care.

Two methods exist for computing the EOFs of timeseries. The first constructs a covariance matrix and then solves the eigenvalue problem to establish eigenvalues and eigenvectors. The second approach uses singular value decomposition (SVD) of the data matrix to obtain eigenvalues, eigenvectors and time varying amplitudes (principal components). With the latter method large covariance matrices are avoided, and it is generally a faster and more stable method. A brief description of the SVD method is given below.

Singular Value Decomposition

Using matrix notation any $M \times N$ matrix A can be factored into

$$A = UIV^T \quad (1)$$

where the columns of U ($M \times N$) are the eigenvectors AA^T , and the columns of V ($N \times N$) are the eigenvectors $A^T A$. The r singular values on the diagonal of λ are the square roots of the nonzero eigenvalues of both AA^T and $A^T A$. If the mean has been removed from A , AA^T and $A^T A$ represent respectively the temporal and spatial covariance matrices. U and V are orthonormal so that

$$U^T U = I \quad (2)$$

$$V^T V = I \quad (3)$$

Suppose we have a $M \times N$ matrix A with M as time dimension and N as depth dimension. Then the N columns of V are the eigenvectors of the $N \times N$ matrix $A^T A$. Thus these eigenvectors are the EOFs of A . The columns of U are the principal components. The values of U and V are linked by the singular values along the diagonal of λ . These are sometimes called the magnitude of the modes, and they are square roots of the eigenvalues of $A^T A$. Similarly to the covariance matrix approach the original data can often to a good approximation be reconstructed by summing over the first few modes. This is because the magnitude (singular value) of the modes rapidly decreases towards zero.

$$\hat{A}_{ij} = \sum_{k=1}^K U_{ik} \lambda_k V_{jk} \quad (4)$$

where $i=1..M$ and $j=1..N$. The error of this reproduction can be quantified by:

$$e = 1 - \frac{\sum_i \sum_j (\hat{A}_{ij} - A_{ij})^2}{\sum_i \sum_j A_{ij}^2} \quad (5)$$

This is the error in variance between the observed and EOF reproduced data. When applied to current profile data we can use this formula to find the explained variance of every mode for all the depths. An example of this is shown in Figure 4.

EOF ON MEASURED CURRENT PROFILES

In the present study 3 different datasets of measured current profiles are considered at water depths ranging from 750m to 1060m. In general the ADCP current measurements are carried out with durations of approximately one year. Some general information about the datasets is listed in Table 1 below.

Table 1: Information about current datasets applied

Set	Field location	Water depth	No. of depths	No. of profiles	Sampling interval
1	Atlantic Margin	750	7	14351	10 min. average every 30 or 60 min.
2	Atlantic Margin	1060	8	6195	10 min. average every 60 min.
3	Nigeria	995	6	10791	10 min. average every 30 or 60 min.

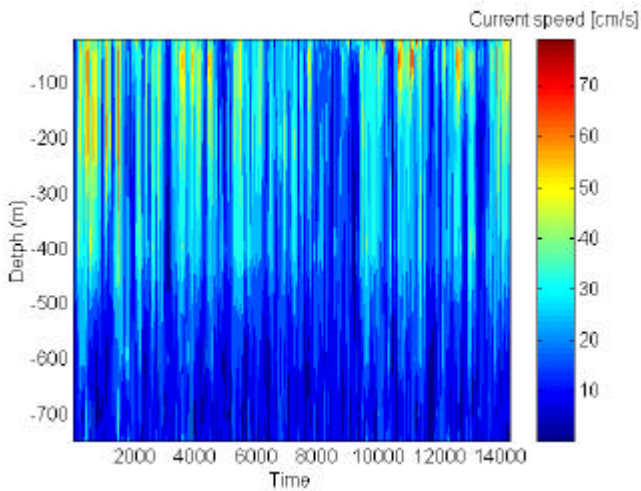


Figure 1: Contour plot of current speeds from dataset 1

A contour plot of the current speeds in dataset 1 is shown in Figure 1. The maximum current speed during the year of data collection is found to be close to 80cm/s. Even though data for current directions are also available, they are neglected in this study for two reasons. First of all, most semi-empirical VIV codes like SHEAR7 and VIVANA can only handle unidirectional current profiles. Secondly, the main emphasis in this study is to compare how well a limited number of EOF current profiles reproduce the current loading from all the measured current profiles with respect to fatigue damage caused by VIV.

Contour plots of the current speed for datasets 2 and 3 are shown in Appendix A - Figure 14 and Figure 15.

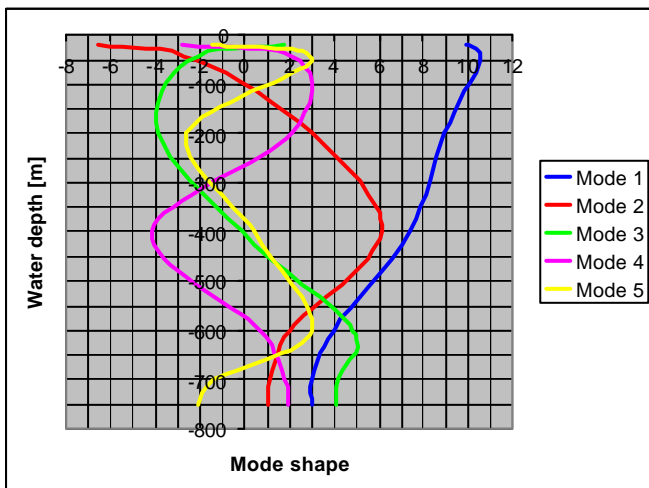


Figure 2: EOF modes for dataset 1

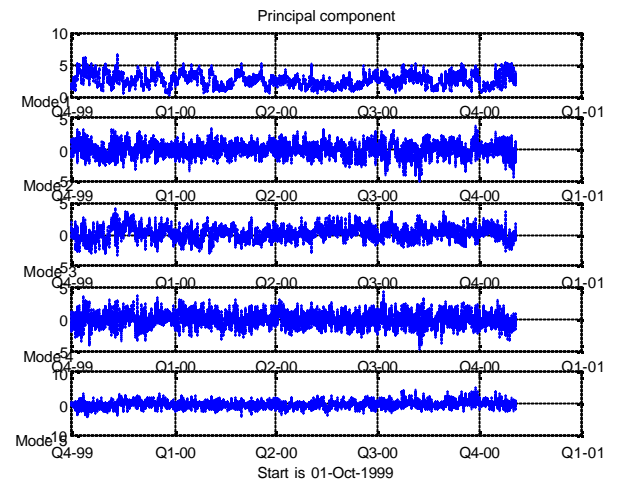


Figure 3: Time history of principal components (here U)

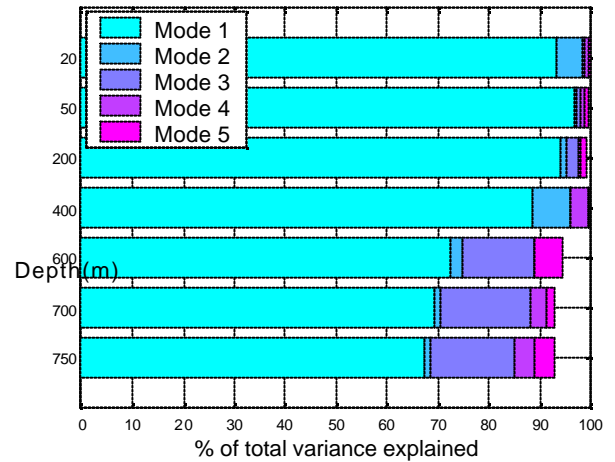


Figure 4: Contribution from the different modes in terms of reproducing the variance in the measured current dataset 1

Applying the SVD technique to dataset 1 gives the EOF modes shown in Figure 2, and the corresponding time histories of the principal components are plotted in Figure 3. As seen in Figure 4, EOF mode 1 reproduces most of the variance in the measured data. For water depths down to 400m, EOF mode 1 covers more than 90% of the variance. Note that 100% means perfect reproduction of the measured data. However, for water depths beyond 400m EOF mode 1 reproduces only around 70% of the variance, while EOF mode 3 becomes increasingly important bringing the percentage of total variance back to approximately 90%. As shown in Figure 4, the contribution from EOF mode 2 at water depths beyond 400m is minor compared to EOF mode 3.

It is also worthwhile to note that both the mode shape of EOF mode 1 and the corresponding principal component are

always positive, while the other mode shapes and principal components are varying between positive and negative values. Hence, the EOF modes beyond mode 1 correct the shape of current profile by adding and subtracting speeds to the current profile given by only EOF mode 1.

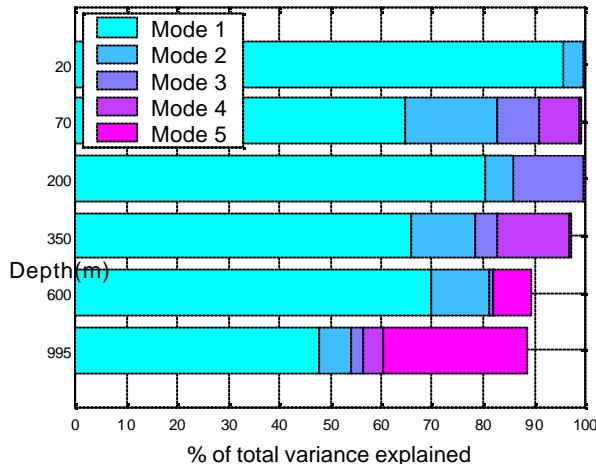


Figure 5: Contribution from the different modes in terms of reproducing the variance in the measured current dataset 3

While applying 3 EOF modes reproduces around 90% of the total variance over the entire water column for dataset 1 and 2 (see Appendix A – Figure 16), the situation is somewhat more complex for dataset 3. As seen in Figure 5 below, EOF mode 1 explains more than 90% of the total variance only for the upper most water depth, and below 50% of the variance for the bottom layer. At the two deepest layers, 5 EOF modes are required in order to bring the percentage of the total variance close to 90%. Hence, the benefit of the EOF method in terms of reducing the complexity of current measurements, is less for dataset 3 than for dataset 1 and 2.

VIV SENSITIVITY TO CURRENT INPUT

A common question related to the use of the EOF method in terms of representing current data, is how much of the total variance in the measurements needs to be reproduced. It may not be 90% as focused upon in the previous section. The missing percentage in variance means that some of the largest peaks in the current measurements are being reproduced with low amplitudes. In this study the aim is to assess what the consequences of underestimating the peaks in current velocity will be to the prediction of riser VIV fatigue damage. Hence, the accumulated VIV fatigue damage has been calculated for all the measured current profiles and compared with the results from the EOF profiles.

Riser model

The riser model applied in the present study is based on a SHEAR7 example model, i.e. riser model number 5. It is a drilling riser with buoyancy modules attached from sea bottom to top-end. In addition the upper 30% of the riser is covered with VIV suppression devices. The original model was for a water depth of 668m, in this study the water depth is adjusted to the actual water depths where the current speeds are measured. The main characteristics of the riser model are listed in Table 2 below, and the most important VIV analyses settings used by SHEAR7 are given in Table 3.

Table 2: Main particulars of the riser models considered

Parameters	Unit	
Buoyancy outer diameter	[m]	1.1303
Pipe outside diameter	[m]	0.5334
Pipe inside diameter	[m]	0.5017
Young’s modulus	[N/m ²]	2.107 x 10 ¹¹
Moment of inertia	[m ⁴]	0.8637 x 10 ⁻³
Mass of pipe	[kg/m]	908
Submerged weight of pipe	[N/m]	1087
Bottom tension	[N]	1.743 x 10 ⁶
Structural damping	[%]	0.3
Suppression device	[%]	30 (upper part)
Water depths	[m]	750, 995, 1060
Number of riser elements	-	226
Boundary conditions	-	Pinned-pinned

Table 3: VIV settings used in the SHEAR7 analyses

Parameters	
Added mass coefficient	1.0
Strouhal number	Curve 200 (rough cylinder)
Single-mode reduced velocity bandwidth	0.5
Multi-mode reduced velocity bandwidth	0.2
Cut-of level participating modes	0.7
Reduction factor of C ₁ for suppression device zones	0.1
SN - curve	E-curve

EOF scatter diagrams

In the papers by Forristall and Cooper (1997) and Jeans and Feld (2001) the main focus was on deriving extreme current profiles. However, Forristall and Cooper (1997) also proposed a method for applying the EOF method in fatigue analyses. Similar to scatter diagrams for significant wave height, H_s, and spectral

peak period, T_p , the amplitudes of the principal components can be combined into bins generating scatter diagrams as shown in Figure 6 below. For each bin there exist current profile determined by the product of the bin's PC amplitude and the EOF eigenvectors. The damage contribution from that bin is then weighted with its occurrence rate.

However, while the wave scatter diagrams usually covers periods of 30 years or more, the current data is usually limited to periods of a year or even less. Hence, the fatigue damage contribution from the most extreme current profiles will be missing in a scatter diagram like the one in Figure 6. One way to include the effects of the most extreme current profiles is to apply the EOF method to establish extreme current profiles and include them in the scatter diagram.

The scatter diagram shown in Figure 6 is established for dataset 1 when 2 EOF modes are considered. It consists of 49 bins where each bin has a probability of occurrence, here given in percent. By including more modes the scatter diagram becomes increasingly complex, i.e. 3 EOF modes give a 3 dimensional scatter diagram where the number of bins increases from 49 to 209 with equal spacing of the PC amplitudes. Going to 5 EOF modes, gives a 5-dimensional scatter diagram consisting of 2175 bins. Hence, the possible benefit of the EOF method decreases rapidly with the number of EOF modes required. The present study focus upon what the required number of EOF modes is in order to replicate the measured current profiles for riser VIV fatigue damage analyses.

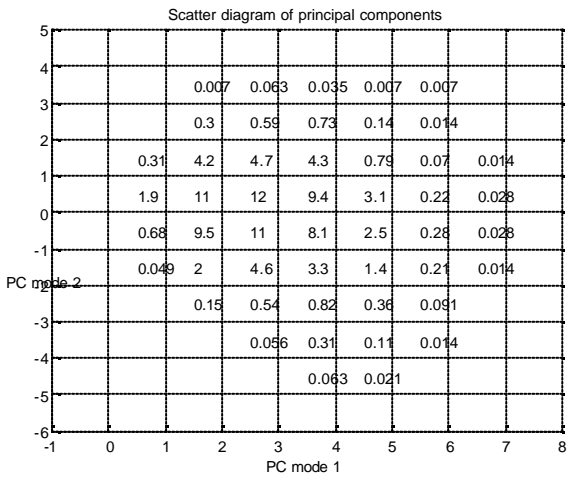


Figure 6: Scatter diagram of the principal components U1 and U2 for dataset 1, i.e. 2 EOF modes are applied. The PC's are grouped into 49 bins, where the numbers in the bins represent percentage of occurrence.

Results from the VIV fatigue damage analyses

In order to evaluate the EOF scatter diagram approach, the “true” VIV fatigue damage has been calculated by accumulating the damage contribution from each of the measured current profiles in a dataset. The accumulated VIV damages predicted by using current profiles from EOF scatter diagrams based upon 2, 3, 4 and 5 EOF modes are then compared as shown in Figure 7.

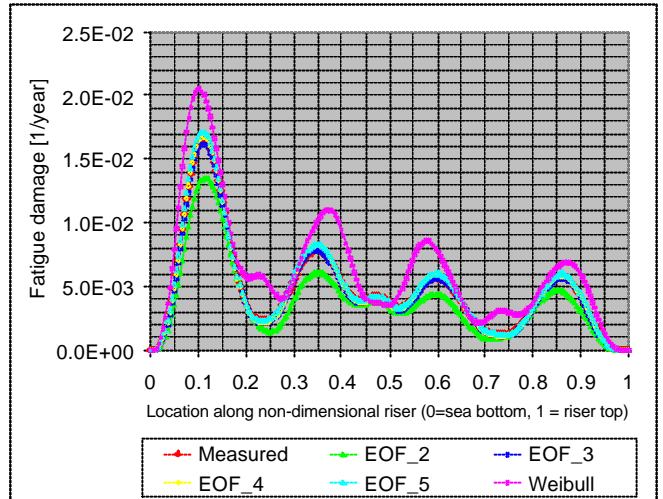


Figure 7: Accumulated VIV fatigue damage along the riser. Here, measured refers to the measured current profiles, EOF_2 ... EOF_5 to number of EOF modes applied to generate the EOF current profiles and Weibull refers to current profiles established by 3-parameter Weibull fit to the measured data.

Here, the accumulated damage along the riser is shown, and the label Weibull refers to VIV fatigue damage predicted by applying current profiles from conventional enveloping techniques, i.e. at each depth of measurements a 3-parameter Weibull distribution is fitted to the measured current speeds. It is anticipated that the datasets represent 1 year of data, hence, 18 current profiles with probability levels of non-exceedance ranging from 0.3 to 1-year level have been applied.

As seen in Figure 7, current profiles based upon 2 EOF cause underestimation of the accumulated VIV fatigue damage - in the order of 20% for the maximum value. Hence, 2 EOF modes do not replicate the measured data accurate enough in this case when focusing on VIV. Adding an EOF mode changes the picture, and an almost perfect match between the curve labeled “measured” and the curve labeled “EOF_3” is seen. Increasing the number of EOF modes to 4 and 5 does not make any difference, i.e. one might conclude that the EOF method has “converged” at 3 modes for this case. The Weibull curve shows that the conventional enveloping method overestimates the fatigue damage by 25% at the maximum value. The shape of the

Weibull damage curve is also somewhat different from the others, indicating that some other eigen modes of the riser have been excited with this approach.

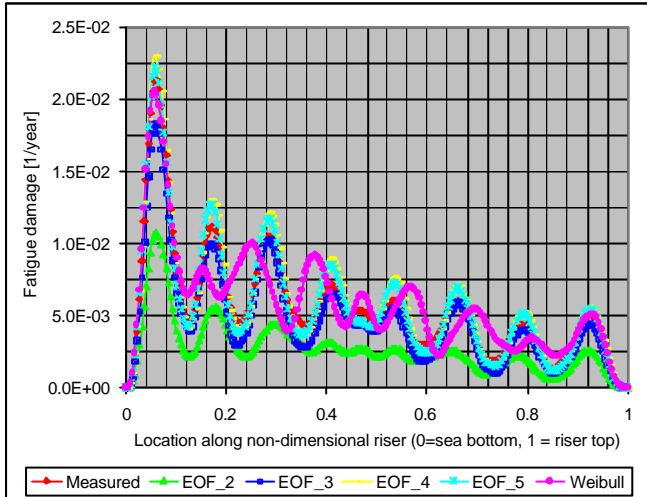


Figure 8: Accumulated VIV fatigue damage along the riser for dataset 2.

The results for dataset 2 are shown in Figure 8. Here, the predictions based upon current profiles generated by 2 EOF modes underestimate the maximum fatigue level even more – in the order of 50%. Adding an EOF mode lifts the fatigue damage level significant, however, 3 EOF modes do not give a perfect match as in the previous case. The maximum peak is underestimated by 14%, but otherwise the match is still very good. Adding 1 or 2 EOF modes in addition brings the maximum fatigue damage level slightly above the level of the “measured” curve – in the order of 5-10%. The “Weibull” curve reproduces the maximum fatigue damage level well, however, the “Weibull” curve shape is again different from the other curves.

It is somewhat surprising that dataset 2 require more EOF modes to match the “measured” curve, than dataset 1. By looking at the variance plots, approximately 90% of the total variance is covered by 2 EOF modes for dataset 2, see Figure 16 (Appendix A), while dataset 1 requires at least 3 modes to be close to cover 90% percent of the total variance, see Figure 4. Hence, one might expect that 2 EOF modes would do the job for dataset 2. One reason why it turns out to be different when it comes to fatigue damage, might be the difference in water depth. Case 2 goes 300m deeper than case 1, hence higher modes might be excited, and higher modes are more sensitive to minor differences in current speed. When comparing Figure 7 and Figure 8 it is obvious that higher modes are excited for dataset 2 than dataset 1.

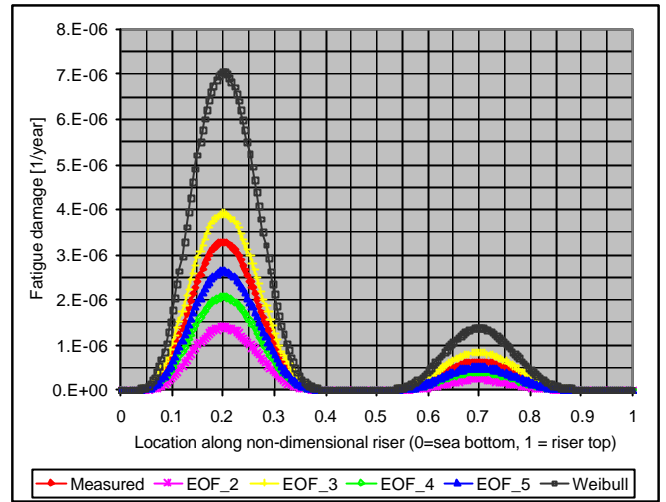


Figure 9: Accumulated VIV fatigue damage along the riser for dataset 3.

The results for dataset 3 are shown Figure 9. This time, all the EOF curves, except “EOF_3”, underestimate the maximum fatigue damage level, while the Weibull approach more and less double the maximum fatigue damage level. It is not unexpected that the fatigue damage level is underestimated for this dataset, since even 5 EOF modes did not manage to explain 90% of the total variance. The reason why the EOF method with 3 modes overestimates the maximum fatigue level is most likely linked to the low current speeds for this dataset, which gives fatigue damage levels 4-orders lower than for dataset 1 and 2. Hence, small changes in current speeds and profile shape may have a significant impact on the overall fatigue damage level. The overestimation by shown by the “EOF_3”-curve in Figure 9, is caused by 2 current profiles out of 120, see Figure 13.

The fatigue damage plots presented so far are all based on EOF scatter diagrams with steps of 1 in PC amplitude. The sensitivity to this step size has been investigated for dataset 1 with 3 EOF modes, changing the step size from 2 to 0.5 in PC amplitude. This change in step sizes brings the number of bins in the EOF scatter diagram from 49 to 923. If 5 EOF modes had been considered, the increase in number of bins with decreasing step sizes would have been even more significant since a 5-dimensional scatter diagram is involved. The results from the sensitivity study are shown in Figure 10 below. It is clearly shown that the two coarsest scatter diagram densities cause overestimations of the VIV fatigue damage level, while step sizes of 1.0 and 0.5 reproduces the “measured” curve very well.

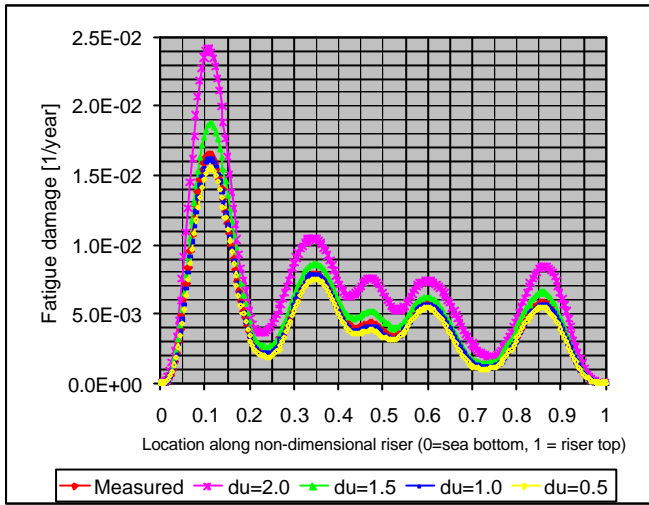


Figure 10: Accumulated VIV fatigue damage along the riser for different scatter diagram densities (3 EOF modes, dataset 1).

Even though the original number of current profiles has been significantly reduced, e.g. from 14351 to 209 profiles for dataset, approximately 200 current profiles may still be too many. For wave scatter diagrams it is common to group the bins into larger blocks, which are properly weighted and applied in the riser analysis.

To assess how many current profiles out of 209 are actually contributing to the overall fatigue damage, the maximum fatigue damage for each bin has been predicted and plotted versus bin number, see Figure 11. To evaluate the accuracy of EOF current profiles on bin level, the accumulated fatigue damage from measured current profiles belonging to a bin has also been calculated for each bin and the maximum values are plotted in Figure 11. Figure 12 is included to illustrate the involved current profiles for one bin, here represented by bin 191 where 15 measured current profiles occur. Hence, by accumulating the VIV fatigue damage predicted for all 15 current profiles and then finding the maximum value, the point for EOF group 191 for the “measured” curve in Figure 11 is found. The corresponding point on the “EOF_3” curve is simply the maximum fatigue damage found when running SHEAR7 with the EOF current profile shown in Figure 12.

As seen in Figure 11, only a limited number of the current profiles contribute to the fatigue damage. For this dataset 12 profiles generate more than 50% of the total fatigue damage, and 45 profiles 93%. Typically, the bins with highest occurrence rate and the bins with highest U1 amplitudes dominate the damage contribution. Hence, combining bins into larger blocks should be a possible strategy. However, SHEAR7 simulations take only a few seconds on a standard PC requiring only a few minutes in total simulation time for 209 different current profiles.

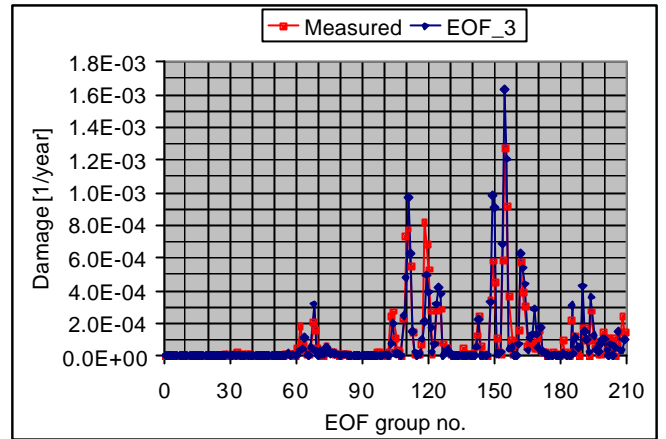


Figure 11: Maximum VIV fatigue damage for each EOF current profile compared with the maximum of the accumulated damage for the corresponding bin of measured profiles (3 EOF modes – dataset 1).

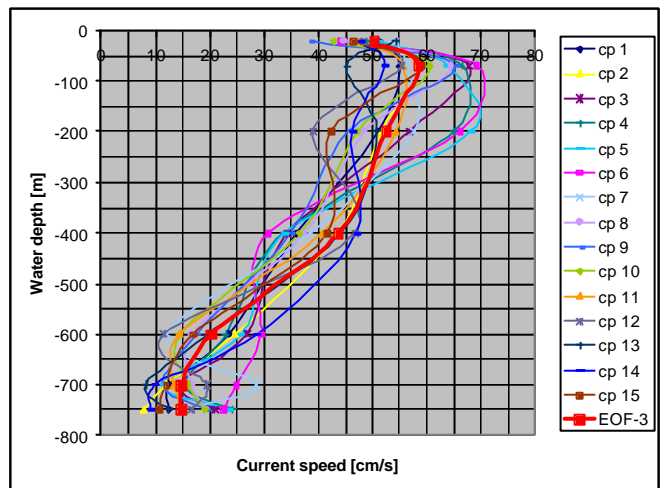


Figure 12: Measured current profiles that belong to bin 191, 15 in total, compared with the corresponding EOF current profile (red line) for bin 191

In Figure 9 it was shown that the EOF method with 3 modes generated current profiles that caused an accumulated VIV fatigue damage that exceeded the damage level of the “measured” curve, while the EOF method 2, 4 and 5 modes generated current loadings that significantly underestimated the VIV fatigue damage. As mentioned earlier, a likely reason why the “EOF_3” curve in Figure 9 does not follow the trend of the other EOF curves, is that at these low current speeds and damage levels the VIV predictions are very sensitive to small changes in current speeds and profile shape. This is clearly shown in Figure 13, where especially one EOF current profile

causes VIV fatigue damage that exceeds the absolute maximum level on the “measured” curve with more than 400%.

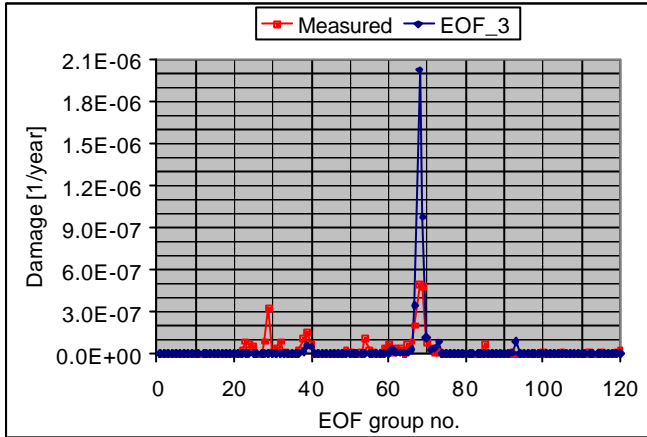


Figure 13: Maximum VIV fatigue damage for each EOF current profile compared with the maximum of the accumulated damage for the corresponding bin of measured profiles (3 EOF modes – dataset 3).

CONCLUSIONS

In the present study it has been shown that the EOF current scatter diagram approach can be a powerful tool to simplify huge amounts of current data from field measurements. A limited set of current profiles with a certain probability can be obtained by organizing the combined amplitudes of the principal components into bins that generate a scatter diagram of the current data.

The accuracy of the EOF scatter diagram approach depends on the size of the bins in terms of step sizes in PC amplitudes and number of EOF modes applied. It has been shown that a step size of 1 in PC amplitude is the best choice for the current datasets considered in this study.

The required number of EOF modes might be coupled to what percentage of total variance of the current data that the EOF modes applied replicate. The datasets causing most fatigue damage in this study are set 1 and 2. For these datasets, the EOF method with 3 modes applied covers almost 90% of the total variance. The corresponding 3-dimensional EOF scatter diagrams consist of approximately 200 bins of combined PC amplitudes generating current profiles for the VIV analyses. The accumulated fatigue damage from the EOF current scatter diagram approach compares very well with the reference curve (accumulated damage from all measured current profiles), both in terms of level and shape. For dataset 1 the match is almost perfect.

For dataset 3 more than 5 EOF modes are required to bring the percentage of total variance close to 90%, increasing the number of bins in the scatter diagram to more than 1000. Even with 5 EOF modes applied the fatigue damage level is underestimated. However, dataset 3 is a low current speed case generating little fatigue damage. Hence, small changes in current profile and current speeds might be the difference between VIV and no VIV.

It is also found that the dominating bins in the EOF scatter diagram with respect to fatigue damage, are the ones with highest occurrence rate and the ones with largest amplitude of principal component 1.

If 90% of the total variance of the current is close to a target for the EOF method when VIV fatigue damage is considered, needs to be further investigated by considering more current datasets.

ACKNOWLEDGMENTS

Statoil is acknowledged for the permission to publish this study.

REFERENCES

Adams, A.J. and Thorogood, J.L. (1998): “*On the choice of current profiles for deep-water riser design*”, SPE Annual Technical Conference and Exhibition, New Orleans.

Forristall, G. Z. and Cooper, C. K. (1997) “*Design current profiles using empirical orthogonal function (EOF) and inverse FORM methods*”, OTC, Houston.

Jeans, R. G. and Feld, G. (2001): “*A method for deriving extreme current profiles to support design of deep water drilling risers*”, Proceedings of OMAE’01/OFT-1181, Rio de Janeiro, Brazil.

Vandiver, J. K, Lee, L. and Leverette, S. (2002): “User guide for SHEAR7 – Version 4.2”, MIT, Cambridge

APPENDIX A – FIGURES FROM DATASET 2 AND 3

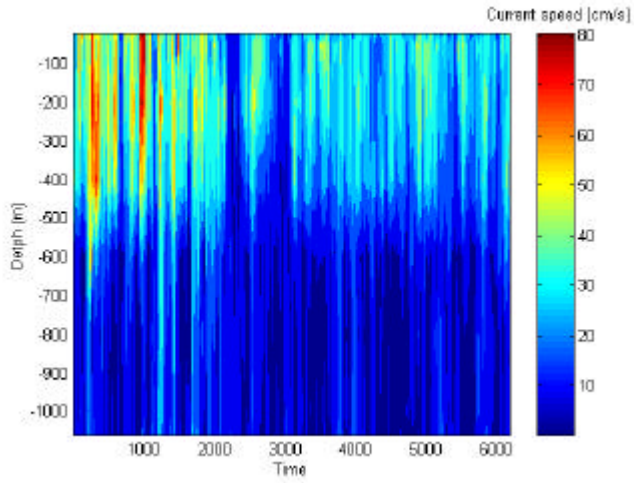


Figure 14: Contour plot of current speeds from dataset 2

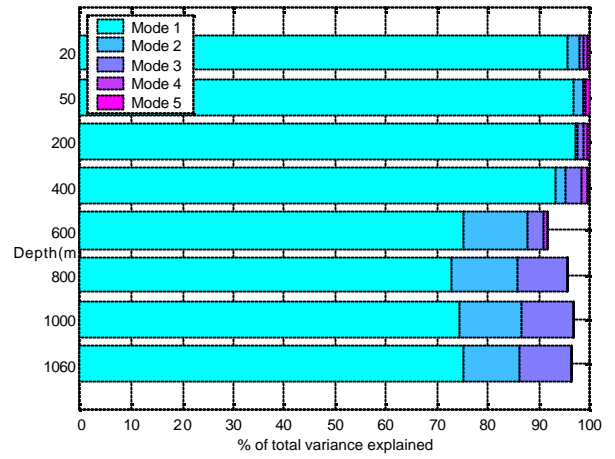


Figure 16: Contribution from the different modes in terms of reproducing the variance in the measured current dataset 2

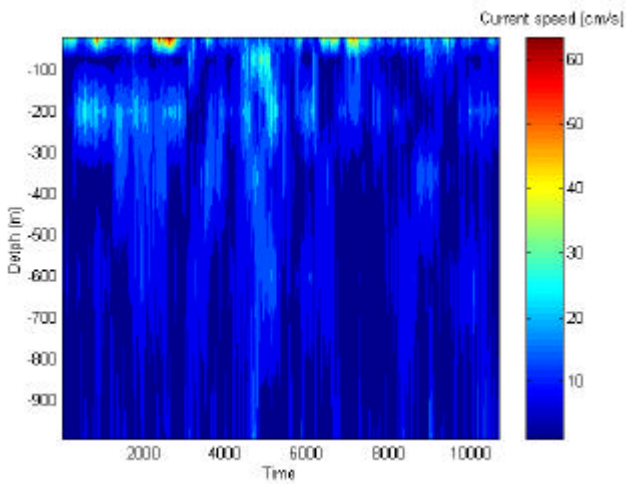


Figure 15: Contour plot of current speeds from dataset 3